Chapter 10
Solutions of Exercises

10.1 Chapter One

1.1 Let us inspect the contribution of the contact force $\boldsymbol{t}$. With the help of (1.67) one has

$$\int_S \boldsymbol{t}\, dS = -\int_S p\boldsymbol{n}\, dS + \boldsymbol{F} \;, \tag{10.1}$$

where $\boldsymbol{F}$ is the shearing force exerted by the plate on the fluid. Indeed the shear contributions vanish on the vertical lines AB, CD and on BC of Fig. 10.1. On the closed surface S, the pressure is uniform and then, $-\int_S p\boldsymbol{n}\, dS = 0$. The integral equation (1.125) becomes

$$\boldsymbol{F} = \rho \int_S (\boldsymbol{v}\cdot\boldsymbol{n})\boldsymbol{v}\, dS \;. \tag{10.2}$$

We need to compute $F = \boldsymbol{F}\cdot\boldsymbol{e}_1$. Therefore from (10.2) one obtains

$$F = \rho \int_S (\boldsymbol{v}\cdot\boldsymbol{n}) v_1\, dS \;. \tag{10.3}$$

With the control volume of thickness Z in x_3 direction exhibited in Fig. 10.1, it is easy to proceed further

$$\rho \int_S (\boldsymbol{v}\cdot\boldsymbol{n})\, v_1\, dS = \rho \sum_{i=1}^{i=6} \int_{S_i} (\boldsymbol{v}\cdot\boldsymbol{n})_i v_1\, dS_i \;. \tag{10.4}$$

In section S_2 the velocity profile is

$$\begin{aligned} v_1(x_2) &= U x_2/h, \text{ for } 0 \le x_2 \le h, \\ v_1 &= U, \text{ for } h \le x_2 \le H \;. \end{aligned} \tag{10.5}$$

M. O. Deville, *An Introduction to the Mechanics of Incompressible Fluids*,
https://doi.org/10.1007/978-3-031-04683-4_10

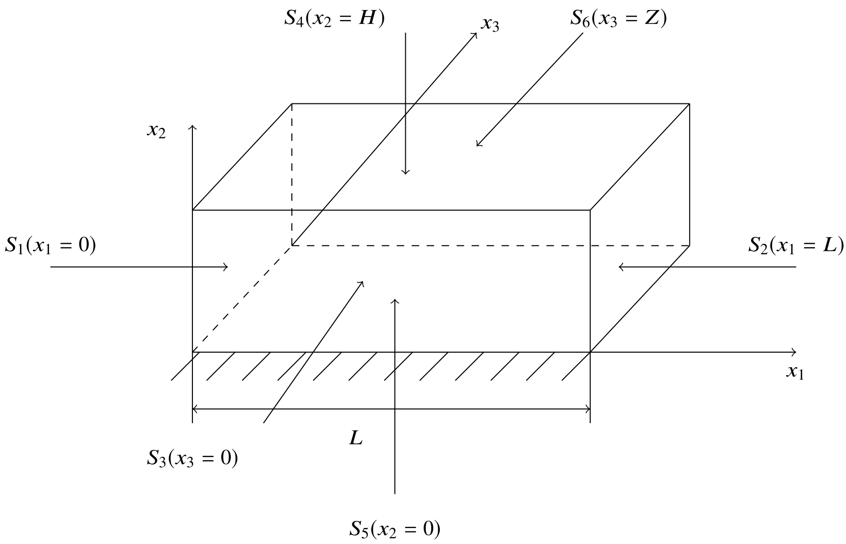

Fig. 10.1 Control volume for the flat plate problem

We have successively

$$\rho \int_{S_1} (\boldsymbol{v} \cdot \boldsymbol{n})_1 v_1 \, dS_1 = -\rho U^2 H Z \quad \boldsymbol{n} = (-1, 0, 0) \quad \boldsymbol{v} = (U, 0, 0)$$

$$\rho \int_{S_2} (\boldsymbol{v} \cdot \boldsymbol{n})_2 v_1 \, dS_2 = \rho U^2 \left((H - h) Z + \frac{hZ}{3} \right) \quad \boldsymbol{n} = (1, 0, 0) \quad \boldsymbol{v} = (v_1(x_2), 0, 0)$$

$$\rho \int_{S_3} (\boldsymbol{v} \cdot \boldsymbol{n})_3 v_1 \, dS_3 = 0 \quad \text{as } (\boldsymbol{v} \cdot \boldsymbol{n})_3 = 0$$

$$\rho \int_{S_4} (\boldsymbol{v} \cdot \boldsymbol{n})_4 v_1 \, dS_4 = \rho \int_0^L U v_2 Z \, dx_1 \quad \boldsymbol{n} = (0, 1, 0) \quad \boldsymbol{v} = (0, v_2, 0) \; .$$

It is forbidden to impose v_2 to be zero on S_4. The fluid flows in the vertical direction through S_4 as the flow rate in the exit S_2 is less than in the entry section S_1. The two last integrals yield $\rho \int_{S_5} (\boldsymbol{v} \cdot \boldsymbol{n})_5 v_1 \, dS_5 = \rho \int_{S_6} (\boldsymbol{v} \cdot \boldsymbol{n})_6 v_1 \, dS_6 = 0$ as the velocity has no component in x_3 direction.

One deduces that

$$F = \rho \int_0^L U v_2 Z \, dx_1 - \frac{2}{3} \rho U^2 h Z \; . \tag{10.6}$$

To evaluate the integral in (10.6) the control volume method is applied to the mass conservation law (1.120)

$$\rho \int_S \boldsymbol{v} \cdot \boldsymbol{n}\, dS = \rho \sum_{i=1}^{i=6} (\boldsymbol{v} \cdot \boldsymbol{n})_i\, dS_i \ . \tag{10.7}$$

We obtain

$$\begin{aligned}
\rho \int_{S_5} (\boldsymbol{v} \cdot \boldsymbol{n})_5\, dS_5 &= \rho \int_{S_6} (\boldsymbol{v} \cdot \boldsymbol{n})_6\, dS_6 = \rho \int_{S_3} (\boldsymbol{v} \cdot \boldsymbol{n})_3\, dS_3 = 0 \\
\rho \int_{S_1} (\boldsymbol{v} \cdot \boldsymbol{n})_1\, dS_1 &= -\rho U H Z \\
\rho \int_{S_2} (\boldsymbol{v} \cdot \boldsymbol{n})_2\, dS_2 &= \rho U \left((H - h) Z + \frac{hZ}{2} \right) \\
\rho \int_{S_4} (\boldsymbol{v} \cdot \boldsymbol{n})_4\, dS_4 &= \rho \int_0^L v_2 Z dx_1 \ .
\end{aligned}$$

Therefore one has

$$\rho \int_0^L v_2 Z dx_1 = \rho U \frac{hZ}{2} \tag{10.8}$$

Combining (10.6) and (10.8), the force F acting by the plate on the fluid is

$$F = -\frac{1}{6} \rho U^2 h Z \ . \tag{10.9}$$

1.2 Incompressibility requires $\nabla \cdot \boldsymbol{v} = 0$. Applying $\partial / \partial x_i$ to the velocity field, one has

$$\begin{aligned}
\frac{\partial v_i}{\partial x_i} &= \frac{A r^3 \delta_{ii} - 3 A r^2 x_i \frac{\partial r}{\partial x_i}}{r^6} \\
&= \frac{A r^3 \delta_{ii} - 3 A r^2 x_i \frac{x_i}{r}}{r^6} \\
&= 0
\end{aligned}$$

since $x_i x_i = r^2$.

It is also possible to solve the problem by computing

$$\begin{aligned}
\operatorname{div} \boldsymbol{v} = \frac{\partial v_i}{\partial x_i} &= A \frac{\partial}{\partial x_i} \left(x_i (x_j x_j)^{-3/2} \right) \\
&= A \left(\delta_{ii} (x_j x_j)^{-3/2} - \frac{3}{2} x_i \cdot 2 (x_j x_j)^{-5/2} x_j \delta_{ji} \right) \\
&= A \left(\delta_{ii} (x_j x_j)^{-3/2} - \frac{3}{2} x_j \cdot 2 (x_j x_j)^{-5/2} x_j \right) = 0 \ ,
\end{aligned}$$

as $\delta_{ii} = 3$.

1.3 The incompressibility equation in cylindrical coordinates (A.2) is written as

$$\frac{1}{r}\frac{\partial(rv_r)}{\partial r}+\frac{1}{r}\frac{\partial v_\theta}{\partial\theta}+\frac{\partial v_z}{\partial z}=0\ .$$

It is easily deduced that the given velocity field is incompressible.

1.4 **Natural Convection between two parallel planes**

The $2D$ velocity field is such that $\boldsymbol{v}=(v_1(x_1,x_2),v_2(x_1,x_2),0)$. However the flow is invariant with respect to translation in the x_2 direction. Therefore it depends only on the x_1 coordinate. With the incompressibility condition (1.115),

$$\frac{\partial v_1}{\partial x_1}=0\ . \tag{10.10}$$

As $v_1=0$ at the walls, $v_1=0$ and $\boldsymbol{v}=(0,v_2,0)$. The temperature gradient is oriented in the horizontal direction, so that the temperature field is such that $T=T(x_1)$. The temperature Eq. (1.117) becomes

$$\frac{d^2T}{dx_1^2}=0\ . \tag{10.11}$$

Integrating with the boundary conditions $T=T_2$ at $x_1=-h$ and $T=T_1$ at $x_1=h$ yields

$$T=-\frac{T_2-T_1}{2h}x_1+\frac{T_1+T_2}{2}:=Ax_1+\frac{T_1+T_2}{2}\ . \tag{10.12}$$

The momentum equation (1.116) gives

$$-\frac{\partial p}{\partial x_2}+\mu\frac{d^2v_2}{dx_1^2}-\rho_0\,g\,(1-a(T-T_0))=0\ . \tag{10.13}$$

The reference temperature is chosen as the mean temperature $T_0=(T_1+T_2)/2$. The flow is not driven by an exterior pressure gradient; then the pressure is purely hydrostatic and results from the integration of

$$-\frac{\partial p}{\partial x_2}-\rho_0\,g=0\ , \tag{10.14}$$

valid at equilibrium. Consequently the velocity field is driven by the buoyancy forces and one solves

$$\mu\frac{d^2v_2}{dx_1^2}+\rho_0\,g\alpha Ax_1=0\ . \tag{10.15}$$

With the boundary conditions $v_2=0$ at $x_1\pm h$,

$$v_2 = -\frac{g\alpha A}{6\nu} x_1(x_1^2 - h^2) = \frac{g\alpha}{12\nu h}(T_1 - T_2)x_1(x_1^2 - h^2) \ . \tag{10.16}$$

It is a simple check to verify that this velocity profile corresponds to a vanishing flow rate across each horizontal cross section.

1.5

- The continuity equation applied to the control volume in dashed lines (Fig. 1.14) yields

$$\int_0^{R_0} v_z(r)\, 2\pi r dr = V\pi R_1^2 \ . \tag{10.17}$$

Using (1.126) in (10.17) one has

$$2v_{max} \int_0^{R_0} \left(1 - \frac{r^2}{R_0^2}\right) r\, dr = V R_1^2 \ . \tag{10.18}$$

Carrying through the integration we obtain

$$\frac{V}{v_{max}} = \frac{1}{2}\frac{R_0^2}{R_1^2} \ . \tag{10.19}$$

- The momentum equation in integral form is applied to the control volume

$$\int_S \rho(\boldsymbol{v}\cdot\boldsymbol{n})\boldsymbol{v} dS = 0 \ . \tag{10.20}$$

Indeed the contact force $\boldsymbol{t} = \boldsymbol{0}$ as there is no diffusion and the pressure is constant and equal to the atmospheric pressure. Consequently one writes successively

$$\begin{aligned}
\int_0^{R_0} (v_z(r) dS) v_z(r) &= \pi V^2 R_1^2 \ , \\
v_{max}^2 \int_0^{R_0} \left(1 - \frac{r^2}{R_0^2}\right)^2 2\pi r dr &= \pi V^2 R_1^2 \ , \\
2v_{max}^2 \frac{R_0^6}{6} &= V^2 R_1^2 \ , \\
\left(\frac{V}{v_{max}}\right)^2 &= \frac{1}{3}\frac{R_0^2}{R_1^2} \ .
\end{aligned} \tag{10.21}$$

With (10.19) and (10.21) the contraction coefficient is

$$\beta = \frac{R_1^2}{R_0^2} = \frac{3}{4} \ . \tag{10.22}$$

10.2 Chapter Two

2.1 In thermal convection problems there is no reference velocity to be chosen like in aerodynamics where the upstream uniform velocity is a given data of the flow. As it is proposed in the problem statement there are three possible choices for the reference velocity. Note that the dimensional matrix of Table 2.1 is almost identical to the one corresponding to the Boussinesq variables. It is sufficient to add the column corresponding to α with $[\alpha \big| 0\,0\,0\ -1]$.

If ρ, μ, L, T are chosen as primary variables, then the minor is not zero. The first and third dimensionless groups become $\Pi_1 = \nu t/L^2$, $\Pi_3 = \boldsymbol{v}L/\nu$. This shows that the reference velocity is indeed ν/L based on the viscous diffusivity. The alternate choice ρ, k, L, c_p with non zero minor generates $\Pi_1 = \Lambda t/L^2$, $\Pi_3 = \boldsymbol{v}L/\Lambda$.

We resort to the Boussinesq equations given by (1.118) and (1.119).

- Let us now consider the dimensionless Boussinesq equations with the viscous diffusivity as reference velocity. The dimensionless variables are

$$x_i = Lx_i'\ ,\ t = \frac{L^2}{\nu}t'\ ,\ v_i = \frac{\nu}{L}v_i'\ ,\ P' = \frac{\tilde{p}L^2}{\rho\nu^2}\ , T - T_0 = (T_1 - T_0)T'\ .$$

Dropping the primes for ease of notation we obtain

$$\operatorname{div} \boldsymbol{v} = 0, \tag{10.23}$$

$$\frac{D\boldsymbol{v}}{Dt} = -\nabla P + \triangle\,\boldsymbol{v} + Gr\,T\boldsymbol{g}, \tag{10.24}$$

$$\frac{DT}{Dt} = \frac{1}{Pr}\triangle\,T. \tag{10.25}$$

- Referring to the thermal diffusivity for the reference velocity, the dimensionless variables become

$$x_i = Lx_i'\ ,\ t = \frac{L^2}{\kappa}t'\ ,\ v_i = \frac{\kappa}{L}v_i'\ ,\ P' = \frac{\tilde{p}L^2}{\rho\kappa^2}\ , T - T_0 = (T_1 - T_0)T'\ . \tag{10.26}$$

The dimensionless Boussinesq equations are now

$$\operatorname{div} \boldsymbol{v} = 0, \tag{10.27}$$

$$\frac{D\boldsymbol{v}}{Dt} = -\nabla P + Pr\,\triangle\,\boldsymbol{v} + Ra\,Pr\,T\boldsymbol{g}, \tag{10.28}$$

$$\frac{DT}{Dt} = \triangle\,T. \tag{10.29}$$

- With the reference velocity $U = (g\alpha(T - T_0)L)^{1/2}$ the dimensionless Boussinesq equations are

$$\operatorname{div} \boldsymbol{v} = 0, \tag{10.30}$$

$$\frac{D\boldsymbol{v}}{Dt} = -\nabla P + \frac{Pr}{Pe}\triangle \boldsymbol{v} - Gr\,T\boldsymbol{g}, \tag{10.31}$$

$$\frac{DT}{Dt} = \frac{1}{Pe}\triangle T. \tag{10.32}$$

2.2 Let us define the dimensionless coordinate variable and velocity as follows

$$\eta = \frac{x_1}{h}\,, \quad v_2^* = \frac{v_2 h}{\nu}\,. \tag{10.33}$$

In dimensionless form, the velocity profile (10.16) reads

$$v_2^* = \frac{1}{12} Gr\,\eta\left(\eta^2 - 1\right)\,, \tag{10.34}$$

where Gr is the Grashof number

$$Gr = \frac{g\alpha(T_2 - T_1)h^3}{\nu^2}\,. \tag{10.35}$$

10.3 Chapter Three

3.1 The solutions obtained in (3.7) and (3.19) for the plane Couette and Poiseuille flows, respectively, result from linear differential equations. As the non-linear terms of the Navier–Stokes equations do not intervene in this problem, one invokes the principle of linear superposition and the solution of the combined plane Couette–Poiseuille flow is written as

$$v_1 = -\frac{h^2}{2\mu}\frac{dP}{dx_1}\frac{x_2}{h}(1 - \frac{x_2}{h}) + \frac{Ux_2}{h}\,.$$

The shear stress is

$$\sigma_{12} = \mu\frac{dv_1}{dx_2} = -\frac{h}{2}\frac{dP}{dx_1}(1 - \frac{2x_2}{h}) + \frac{\mu U}{h}\,.$$

Finally, the flow rate is

$$Q = \int_0^h v_1\,dx_2 = -\frac{h^3}{12\mu}\frac{dP}{dx_1} + \frac{Uh}{2}\,.$$

3.2 We will refer to the spherical coordinates (r, θ, φ) as in Fig. B.1. The rotation axis of the sphere with the angular velocity $\boldsymbol{\Omega} = \Omega \boldsymbol{e}_{x_3}$ is axis x_3. As a consequence of the problem's symmetries, the velocity field has only one single component such that

$$\boldsymbol{v} = v_\varphi(r, \theta)\boldsymbol{e}_\varphi \, . \tag{10.36}$$

We solve the Stokes equations with the boundary conditions

$$\boldsymbol{v} = 0 \quad \text{in} \quad r = \infty \tag{10.37}$$

$$v_\varphi = \Omega R \sin\theta \quad \text{in} \quad r = R \, . \tag{10.38}$$

The form of the boundary conditions (10.38) suggests to search the solution under the form

$$v_\varphi = \Omega R f(r) \sin\theta \, , \quad p = p_\infty \, . \tag{10.39}$$

One verifies that the mass conservation equation (B.20) is trivially verified by (10.39). The pressure gradient does not intervene in (B.23) because of axial symmetry ($\partial/\partial\varphi = 0$). One has

$$\Delta v_\varphi - \frac{v_\varphi}{r^2 \sin^2\theta} = \Omega R \sin\theta \left(f'' + \frac{2f'}{r} - \frac{2f}{r^2} \right) = 0 \, . \tag{10.40}$$

The f solution written as $f(r) = \sum_{n=-\infty}^{+\infty} C_n r^n$ gives

$$f(r) = C_1 r + \frac{C_2}{r^2} \, . \tag{10.41}$$

The boundary conditions (10.37) and (10.38) impose $C_1 = 0$ and $C_2 = R^2$, respectively. The velocity field around the rotating sphere is

$$v_\varphi = \Omega \frac{R^3}{r^2} \sin\theta \, \boldsymbol{e}_\varphi \, .$$

3.3 **Spherical Couette flow**

The boundary conditions are

$$v_\varphi = \Omega_1 R_1 \sin\theta \quad \text{in} \quad r = R_1 \tag{10.42}$$

$$v_\varphi = \Omega_2 R_2 \sin\theta \quad \text{in} \quad r = R_2 \, . \tag{10.43}$$

The considerations of the previous exercise remain valid for the velocity profile search under the form (10.39)

$$v_\varphi = f(r) \sin\theta \, , \quad p = p_\infty \, . \tag{10.44}$$

We will note that we do not use anymore the factor ΩR, as now we have two radii and two angular velocities to take care of. The equation to solve is thus

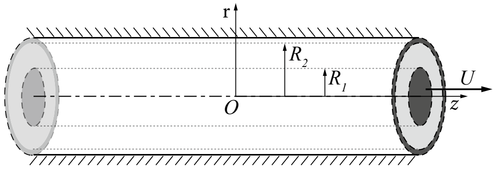

Fig. 10.2 Flow between two concentric cylinders, one fixed and the other moving with velocity U in the z direction

$$\Delta v_\varphi - \frac{v_\varphi}{r^2 \sin^2\theta} = \sin\theta\left(f'' + \frac{2f'}{r} - \frac{2f}{r^2}\right) = 0\,, \tag{10.45}$$

whose solution is

$$f(r) = C_1 r + \frac{C_2}{r^2}\,. \tag{10.46}$$

The imposition of the boundary conditions (10.42) and (10.43) yields

$$C_1 = \frac{\Omega_2 R_2^3 - \Omega_1 R_1^3}{R_2^3 - R_1^3}, \quad C_2 = \frac{\Omega_1 - \Omega_2}{R_2^3 - R_1^3} R_1^3 R_2^3\,. \tag{10.47}$$

3.4 We work in cylindrical coordinates with the z axis in the direction of the axes of both cylinders (cf. Fig. 10.2). The only non zero velocity component is clearly v_z. Moreover $v_z = v_z(r)$.

The flow is kinematically forced by the displacement of the inner cylinder. No pressure gradient is involved in the fluid motion.

Equation (A.23) gives

$$\frac{1}{r}\frac{d}{dr}\left(r\frac{dv_z}{dr}\right) = 0\,. \tag{10.48}$$

Integrating (10.48), one finds

$$v_z = C_1 \ln r + C_2\,. \tag{10.49}$$

The boundary conditions are

$$v_z(r = R_1) = U \tag{10.50}$$

$$v_z(r = R_2) = 0\,. \tag{10.51}$$

Imposing (10.50) and (10.51) to (10.49), one obtains the velocity field

$$v_z = \frac{U}{\ln\frac{R_1}{R_2}} \ln\frac{r}{R_2}\,. \tag{10.52}$$

With the help of (A.4), the only non zero component of the stress tensor is σ_{rz} equal to

$$\sigma_{rz} = \mu\left(\frac{\partial v_z}{\partial r} + \frac{\partial v_r}{\partial z}\right) = \mu\frac{U}{\ln\frac{R_1}{R_2}}\frac{1}{r} \; . \tag{10.53}$$

The friction force per unit length acting on the moving cylinder is given by the integral

$$\int_0^1 \sigma_{rz}|_{r=R1} 2\pi R_1 dz = 2\pi\mu\frac{U}{\ln\frac{R_1}{R_2}} \; . \tag{10.54}$$

3.5 Couette flow with a free surface

- It is simple to obtain $B = 0$ and $A = \omega_2$ in the Couette solution (3.41).
- The Navier–Stokes equations involving the pressure contributions are

$$\frac{\partial p}{\partial r} = \rho\,\frac{v_\theta^2}{r} \; , \tag{10.55}$$

$$\frac{\partial p}{\partial z} = -\rho g \; . \tag{10.56}$$

Therefore we conclude that $p = p(r, z)$ and $dp = \frac{\partial p}{\partial r}dr + \frac{\partial p}{\partial z}dz$. As at the free surface $p = p_a = cst$, one has $dp = 0$. Then we obtain

$$\frac{dz}{dr} = -\frac{\frac{\partial p}{\partial r}}{\frac{\partial p}{\partial z}} = -\frac{\rho\,\frac{v_\theta^2}{r}}{-\rho g} = \frac{1}{g}\omega_2^2 r \; . \tag{10.57}$$

Integrating (10.57) one gets

$$z = \frac{1}{2g}\omega_2^2 r^2 + C \; , \tag{10.58}$$

with C a constant. Imposing $z(R_1) = z_1$ we find

$$z = \frac{1}{2g}\omega_2^2(r^2 - R_1^2) + z_1 \; . \tag{10.59}$$

The free surface has a parabolic shape.

3.6 Plane Couette flow with two layers

The flow is two-dimensional and $v_3 = 0$. Furthermore we have $\partial/\partial x_1 = \partial/\partial x_3 = 0$. The two components v_1 and v_2 are only dependent on x_2. The incompressibility constraint imposes that $v_2 = 0$ and $v_1 = v_1(x_2)$. The hypothesis on the pressure gradient implies $\partial p/\partial x_1 = 0$. The Navier–Stokes equations yield

$$\mu \frac{\partial^2 v_1}{\partial x_2^2} = 0$$
$$-\frac{\partial p}{\partial x_2} - \rho g = 0 \tag{10.60}$$
$$-\frac{\partial p}{\partial x_3} = 0 \,.$$

In the two layers labeled 1 and 2 by upper indices we have

$$\frac{\partial^2 v_1}{\partial x_2^2} = 0$$
$$\frac{dp}{dx_2} + \rho g = 0 \,. \tag{10.61}$$

Integrating we obtain

$$\begin{aligned} v_1^1 &= A_1 x_2 + B_1, \quad p^1 = -\rho_1 g x_2 + C^1 \\ v_1^2 &= A_2 x_2 + B_2, \quad p^2 = -\rho_2 g x_2 + C^2 \,. \end{aligned} \tag{10.62}$$

The boundary conditions are $v_1^1(h_1) = U$ and $v_1^2(-h_2) = 0$. We have

$$A_1 h_1 + B_1 = U \tag{10.63}$$
$$-A_2 h_2 + B_2 = 0 \,. \tag{10.64}$$

As the two fluids do not slip at the interface, one gets

$$B_1 = B_2 \,. \tag{10.65}$$

The interface is in equilibrium and the contact forces satisfy Eq. (1.76). With $\boldsymbol{n}_{\mathrm{I}} = \boldsymbol{e}_2$, the unit vector in direction x_2, we have

$$\boldsymbol{\sigma}^1 \boldsymbol{e}_2 = \boldsymbol{\sigma}^2 \boldsymbol{e}_2 \,. \tag{10.66}$$

In terms of stress components, relation (10.66) yields

$$\sigma_{12}^1 = \sigma_{12}^2, \quad \sigma_{22}^1 = \sigma_{22}^2, \quad \sigma_{32}^1 = \sigma_{32}^2 \,. \tag{10.67}$$

With the definition of the constitutive equation (1.67), the stress components in (10.67) are

$$\sigma^1_{12} = 2\mu_1 d^1_{12} = \mu_1 \frac{dv^1_1}{dx_2} = \mu_1 A_1 \tag{10.68}$$

$$\sigma^2_{12} = 2\mu_2 d^2_{12} = \mu_2 \frac{dv^2_1}{dx_2} = \mu_2 A_2 \tag{10.69}$$

$$\sigma^1_{22} = -p^1 + 2\mu_1 d^1_{22} = -p^1 \tag{10.70}$$

$$\sigma^2_{22} = -p^2 \tag{10.71}$$

$$\sigma^1_{32} = \sigma^2_{32} = 0\,. \tag{10.72}$$

The first condition on the stress components (10.67) imposes

$$\mu_1 A_1 = \mu_2 A_2\,. \tag{10.73}$$

The second condition produces $-p^1 = -p^2$ at $x_2 = 0$ and then $C_1 = C_2 = p_0$ the pressure at the interface. Using (10.63)–(10.65) and (10.73) we obtain

$$A_1 = \frac{\mu_2 U}{\mu_2 h_1 + \mu_1 h_2} \tag{10.74}$$

$$A_2 = \frac{\mu_1 A_1}{\mu_2} = \frac{\mu_1 U}{\mu_2 h_1 + \mu_1 h_2} \tag{10.75}$$

$$B_2 = B_1 = \frac{\mu_1 h_2 U}{\mu_2 h_1 + \mu_1 h_2}\,. \tag{10.76}$$

The velocity components and pressures are

$$v^1_1 = \frac{(\mu_2 x_2 + \mu_1 h_2)U}{\mu_2 h_1 + \mu_1 h_2}, \quad p^1 = -\rho_1 g x_2 + p_0 \tag{10.77}$$

$$v^2_1 = \frac{(\mu_1 x_2 + \mu_1 h_2)U}{\mu_2 h_1 + \mu_1 h_2}, \quad p^2 = -\rho_2 g x_2 + p_0\,. \tag{10.78}$$

Note that if $h_2 = 0$, we recover the velocity profile of the standard plane Couette flow.

The vorticity is orthogonal to the plane of flow and $\omega_3 = -dv_1/dx_2$. We have

$$\omega^1_3 = -\frac{\mu_2 U}{\mu_2 h_1 + \mu_1 h_2} = cst \tag{10.79}$$

$$\omega^2_3 = -\frac{\mu_1 U}{\mu_2 h_1 + \mu_1 h_2}\,. \tag{10.80}$$

3.7 **Bubble dynamics**

The spherical symmetry of the physical situation makes it convenient to work with a spherical coordinate system with origin at the center of the bubble as is shown in Fig. 10.3. All derivatives with respect to θ and φ vanish. It is obvious that the only velocity component relevant to the problem is v_r and $v_r = v_r(r, t)$. The continuity

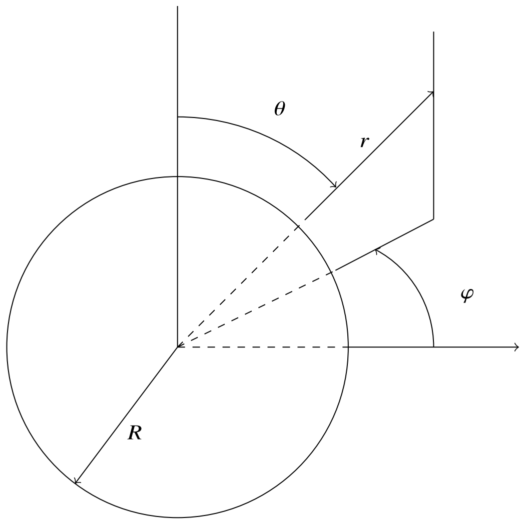

Fig. 10.3 Bubble geometry and associated spherical coordinates

equation and the Navier–Stokes equation for v_r give with the help of relations (B.20) and (B.21)

$$\frac{1}{r^2}\frac{\partial}{\partial r}(r^2\, v_r) = 0 \tag{10.81}$$

$$\rho\left(\frac{\partial v_r}{\partial t} + v_r\frac{\partial v_r}{\partial r}\right) = -\frac{\partial p}{\partial r} + \mu\left(\frac{1}{r^2}\frac{\partial}{\partial r}(r^2\frac{\partial v_r}{\partial r}) - \frac{2v_r}{r^2}\right)\ . \tag{10.82}$$

The integration of (10.81) gives $v_r = A/r^2$. With the boundary condition $v_r = \dot{R}$ at the bubble wall, $\dot{R}$ denoting the wall velocity, we obtain $A = R^2\dot{R}$. The dot denotes the time derivative. Then we have

$$v_r = \frac{\dot{R}R^2}{r^2}\ . \tag{10.83}$$

Inserting (10.83) in (10.82) we have

$$-\frac{\partial p}{\partial r} = \rho\left(2\frac{R\dot{R}^2}{r^2} + \frac{R^2\ddot{R}}{r^2} - 2\frac{R^4\dot{R}^2}{r^5}\right)\ . \tag{10.84}$$

Notice that the viscous term disappears by cancellation. We will integrate (10.84) from the bubble boundary $r = R$ to infinity $r \to \infty$. We obtain

$$-\frac{1}{\rho}\int_{p(R)}^{p(\infty)} dp = \int_R^{\infty}\left(\frac{1}{r^2}\left[2R\dot{R}^2 + R^2\ddot{R}\right] - 2\frac{R^4\dot{R}^2}{r^5}\right) dr\ . \tag{10.85}$$

Carrying the algebra further we get

$$\frac{p(R)-p_\infty}{\rho} = \left[-\frac{1}{r}\left[2R\dot{R}^2 + R^2\ddot{R}\right] + \frac{R^4\dot{R}^2}{2r^4}\right]_R^\infty$$
$$= R\ddot{R} + \frac{3}{2}\dot{R}^2\,. \tag{10.86}$$

The stress components with the help of relations (B.19)–(B.23) are given by

$$\sigma_{rr} = -p - \frac{4\mu R^2\dot{R}}{r^3} \tag{10.87}$$
$$\sigma_{\theta\theta} = \sigma_{\varphi\varphi} = -p + \frac{2\mu R^2\dot{R}}{r^3} \tag{10.88}$$
$$\sigma_{\theta\varphi} = \sigma_{\varphi r} = \sigma_{r\theta} = 0\,. \tag{10.89}$$

Within the bubble

$$\sigma_{rr} = \sigma_{\theta\theta} = \sigma_{\varphi\varphi} = -p_g \tag{10.90}$$
$$\sigma_{\theta\varphi} = \sigma_{\varphi r} = \sigma_{r\theta} = 0\,. \tag{10.91}$$

The stress components $\sigma_{\phi r}$ and $\sigma_{r\theta}$ must be continuous across the bubble surface. The comparison of (10.89) with (10.91) reveals that this requirement is automatically satisfied. The stress component σ_{rr} must experience a jump of magnitude $2\gamma/R$, where γ is the coefficient of interfacial tension (cf. Eq. (1.82)); the stress value inside the bubble is lower. Comparing Eq. (10.87) with (10.90), we find that the pressure just outside the bubble wall is given by

$$p(R+\varepsilon, t) = p_g(t) - \frac{(2\gamma + 4\mu\dot{R})}{R}, \quad \varepsilon \ll 1\,. \tag{10.92}$$

Setting $r = (R+\varepsilon)$ in Eq. (10.86), we obtain an ordinary differential equation for the bubble radius as a function of time:

$$R\ddot{R} + \frac{3}{2}\dot{R}^2 + \frac{4\mu\dot{R}}{\rho R} + \frac{2\gamma}{\rho R} = \frac{p_\infty(t) - p_b}{\rho}\,, \tag{10.93}$$

with p_g the pressure inside the bubble. Since (10.93) is a second-order equation, two initial conditions must be specified. Most simply, $R(0)$ and $\dot{R}(0)$ will be given. Equation (10.93) is the Rayleigh–Plesset equation.

The treatment given here has been restricted to spherical bubbles. In practice, the presence of a unidirectional gravitational field tends to destroy the spherical symmetry. It also causes the bubble to rise in the liquid, and our analysis does not account for streaming past the bubble.

However in certain physical problems the bubble is small enough so that interfacial tension causes it to remain essentially spherical. When streaming past the bubble is negligible, Eq. (10.93) can still be applied. Cavitation bubbles can be treated, but in the literature on cavitation in liquids, viscosity is usually neglected, so that the term $4\mu\dot{R}/\rho R$ is dropped from Eq. (10.93).

10.4 Chapter Four

4.1 The solution of the circular Couette flow is given by Eq. (3.41). Then $\boldsymbol{v} = (0, v_\theta(r), 0)$. The vorticity has the components

$$\boldsymbol{\omega} = (0, 0, \frac{1}{r}\frac{\partial}{\partial r}(rv_\theta)) . \tag{10.94}$$

Therefore $\omega_z = 2A$. The vorticity in the circular Couette flow is constant. It is interesting to note that if $B = 0$, i.e. $\omega_1 = \omega_2$, the fluid is in solid rotation and the vorticity value is twice the angular velocity.

Using Stokes theorem (4.4), the surface integral is easily computed as $\boldsymbol{\omega} \cdot \boldsymbol{n} = \omega_z$ and the surface $S = \pi(R_2^2 - R_1^2)$. Therefore $\int_S \boldsymbol{\omega} \cdot \boldsymbol{n}\, dS = 2\pi(R_2^2\omega_2 - R_1^2\omega_1)$. For the line integral, we define a contour made of a straight line orthogonal to the cylinders reaching the two boundary circumferences C_1 (inner) and C_2 (outer) at points L_1 and L_2. The contour is swept from the L_1 to L_2, goes counterclockwise around C_2 till L_2, crosses the annulus from L_2 to L_1 and then circumnavigates clockwise around C_1 until reaching L_1. It is obvious that both integrals on the line segment L_1L_2 do not contribute to the integral as the velocity is orthogonal to the integration path. For the integrals around C_1 and C_2 we have

$$\begin{aligned}
&\oint_{C_1} v_\theta(R_1) r d\theta = \int_0^{2\pi} v_\theta(R_1) R_1 d\theta = -2\pi R_1 v_\theta(R1) = -2\pi R_1^2\omega_1 \\
&\oint_{C_2} v_\theta(R_2) r d\theta = 2\pi R_2^2\omega_2
\end{aligned} \tag{10.95}$$

We conclude that the Stokes theorem is satisfied.

4.2 We consider the streamline SA from the free surface S toward the orifice Or of the enclosure (cf. Fig. 10.4) and we apply to it the Bernoulli theorem (4.41) to obtain

$$p_S + \frac{\rho v_S^2}{2} + \rho\chi_S = p_A + \frac{\rho v_A^2}{2} + \rho\chi_A .$$

By (4.13), one obtains

$$-g = -\frac{\partial\chi}{\partial x_3} ,$$

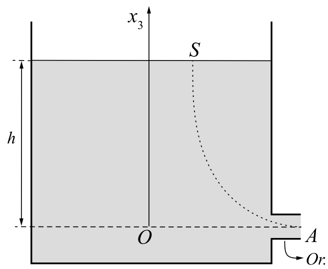

Fig. 10.4 Enclosure with free surface and orifice

and thus $\chi = gx_3 + C$. At the free surface the pressure is that of ambiant air; it is the same situation at the orifice. Therefore $p_S = p_A = p_{air}$. If we set the origin of the x_3 axis at the level of the orifice, the contribution of $\rho\chi$ is equal to C. For the sake of simplicity, we set $C = 0$, while at the free surface $x_3 = h$, $\rho\chi_S = \rho gh$. On the free surface, the velocity v_S is zero (this is especially true when the enclosure is large) and setting $v_A = v$ one has

$$\rho gh = \frac{\rho}{2} v^2 \,. \tag{10.96}$$

This gives the sought relation, which is known as Torricelli formula.

4.3 **Hill's Vortex**

We follow the solution described by Rieutord [79]. Another way of presenting and solving Hill's vortex leading to the same relationships is to be found in the book by Shivamoggi [91].

- Referring to the equations for the **curl** and div in spherical coordinates (Appendix B), the equations **curl** = **0** and div $\boldsymbol{v} = 0$ yield

$$\frac{1}{r}\frac{\partial}{\partial r}(r v_\theta) - \frac{1}{r}\frac{\partial v_r}{\partial \theta} = \frac{\omega r}{R} \sin\theta \tag{10.97}$$

$$\frac{1}{r^2}\frac{\partial}{\partial r}(r^2 v_r) + \frac{1}{r \sin\theta}\frac{\partial(\sin\theta\, v_\theta)}{\partial\theta} = 0 \,. \tag{10.98}$$

Using the suggested form of v_r and v_θ given in the statement, one gets from (10.98)

$$g(r) = -\frac{1}{2r}\frac{d}{dr}(r^2 f) \,. \tag{10.99}$$

Equation (10.97) with the help of Eq. (10.99) leads to relation

$$\frac{d^2}{dr^2}(r^2 f) - 2f = -\frac{2\omega r^2}{R} \,. \tag{10.100}$$

The particular solution f_p of (10.100) is sought as $f_p = Cr^2$ with C a constant. Inserting f_p in (10.100), one obtains $C = -\omega/5R$. The homogeneous solution

f_h gives $f = A/r^3 + B$. The boundary conditions allow the determination of the integration constants. First the velocity must be finite when $r \to 0$. This imposes $A = 0$. Secondly the radial component v_r vanishes for $r = R$. Eventually

$$v_r = \frac{\omega}{5R}(R^2 - r^2)\cos\theta \quad \text{and} \quad v_\theta = \frac{\omega}{5R}(2r^2 - R^2)\sin\theta \,. \tag{10.101}$$

Note that on the sphere the velocity is such that $v_\theta = \omega R \sin\theta/5$.

- Outside the sphere, the flow is irrotational and the velocity comes the velocity potential (4.36), solution of the Laplace equation

$$\Delta\Phi = 0 \,. \tag{10.102}$$

We obtain

$$\Phi(r,\theta) = (Ar + \frac{B}{r^2})\cos\theta \,. \tag{10.103}$$

The boundary conditions are

$$v_r(r = R) = 0, \quad \text{and} \quad v_\theta(r = R) = \omega R \sin\theta/5 \,. \tag{10.104}$$

Imposing (10.104) to (10.103) yields

$$v_r = \frac{2\omega R}{15}\left(-1 + (\frac{R}{r})^3\right)\cos\theta, \quad \text{and} \quad v_\theta = \frac{2\omega R}{15}\left(1 + \frac{1}{2}(\frac{R}{r})^3\right)\sin\theta \,. \tag{10.105}$$

- Introducing the streamfunction ψ such as

$$v_r = \frac{1}{r^2\sin\theta}\frac{\partial\psi}{\partial\theta} \quad \text{and} \quad v_\theta = -\frac{1}{r\sin\theta}\frac{\partial\psi}{\partial r} \,, \tag{10.106}$$

from the velocity components (10.105), the streamfunctions for the full flow are

$$\psi = \frac{\omega r^2}{10R}(R^2 - r^2)\sin^2\theta \quad \text{for} \quad r \le R \tag{10.107}$$

$$\psi = \frac{\omega R r^2}{15}\left(-1 + (\frac{R}{r})^3\right)\sin^2\theta \quad \text{for} \quad r > R \tag{10.108}$$

Figure 10.5 shows the streamlines associated to Hill's vortex in the meridian plane (r, z) of the cylindrical coordinates.

4.4 Drain of a container

- With Eqs. (4.100) and (A.20), it is obvious that div $\boldsymbol{v} = 0$.
- With Eqs. (4.100) and (A.6), we have **curl** $\boldsymbol{\omega} = \mathbf{0}$.
- Using the unperturbed velocity component and the steady state vorticity Eq. (4.24) for ω_z, we obtain

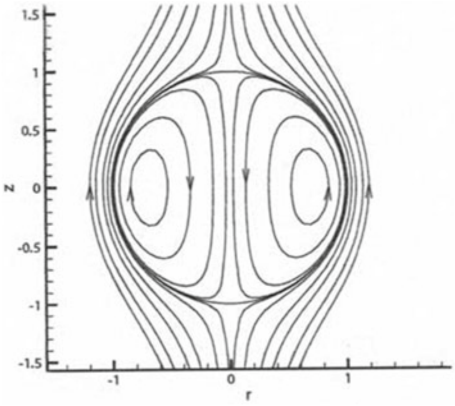

Fig. 10.5 Hill's vortex streamlines

$$\frac{D\omega_z}{Dt} = (\boldsymbol{v} \cdot \nabla)\omega_z = v_r \frac{\partial \omega_z}{\partial r} = \omega_z \frac{\partial v_z}{\partial z} + \frac{\nu}{r}\frac{\partial}{\partial r}\left(r \frac{\partial \omega_z}{\partial r}\right) . \tag{10.109}$$

This relationship yields

$$-\frac{ar}{2}\frac{d\omega_z}{dr} = a\omega_z + \frac{\nu}{r}\frac{d}{dr}\left(r\frac{d\omega_z}{dr}\right) . \tag{10.110}$$

Consequently

$$\frac{d}{dr}\left[\nu\, r \frac{d\omega_z}{dr} + \frac{a}{2}\omega_z r^2\right] = 0 . \tag{10.111}$$

Integration of (10.111) produces (4.101).

- The integration constant must be zero. If this were not the case, the vorticity ω_z would diverge logarithmically at small values of r as the viscous term would dominate the other terms. On the contrary, for large values of r, the viscous term is less influent and the vorticity decays as $1/r^2$. Therefore the total vorticity integrated over the flow volume is blowing up; nonetheless the vorticity must remain finite and constant as there exists no mechanism to create vorticity in this problem.
- With $C = 0$, the integration of (4.101) gives

$$\omega_z = \omega_z\big|_{r=0} \exp\left(-\frac{ar^2}{4\nu}\right) . \tag{10.112}$$

- The result (10.112) shows the presence of a characteristic length $\delta = \sqrt{\nu/a}$.
- Over the distance δ there is an equilibrium between the stretching effects of the elongational velocity field $\boldsymbol{v}$ and the sprawl by viscous diffusion. If the flow occurs through an orifice of diameter d with a reference velocity U, then we have

$$a \simeq \frac{U}{d}\ , \quad \frac{\delta}{d} \simeq \sqrt{\frac{\nu}{Ud}} = Re^{-\frac{1}{2}} \tag{10.113}$$

The higher the value of the Reynolds number, the more concentrated the vorticity in a small diameter core.

4.5 Vortex sheet

- From the problem statement, we have $v_2 = v_3 = 0$ and $v_1 = v_1(x_2, t)$. The non zero vorticity component is $\omega_3(x_2, t) = -\partial v_1/\partial x_2$. As the flow is two-dimensional and the vorticity is orthogonal to the plane flow, the term $(\boldsymbol{\omega} \cdot \nabla)\boldsymbol{v}$ vanishes. The vorticity governing equation (4.24) reduces to

$$\frac{\partial \omega_3}{\partial t} = \nu \frac{\partial^2 \omega_3}{\partial x_2^2}\ . \tag{10.114}$$

- This equation is of diffusion type as was (3.71). We introduce the dimensionless variables

$$\eta = \frac{x_2}{\sqrt{\nu t}} \quad \text{and} \quad \upsilon = \frac{U^2 t}{\nu}\ . \tag{10.115}$$

The vorticity is decomposed by separation of variables

$$\omega_3 = f(\eta) g(\upsilon)\ . \tag{10.116}$$

We have

$$\begin{aligned}
\frac{\partial \omega_3}{\partial t} &= \frac{\partial \eta}{\partial t} f'(\eta) g(\upsilon) + f(\eta) \frac{\partial \upsilon}{\partial t} g'(\upsilon) \\
&= -\frac{\eta}{2t} f'(\eta) g(\upsilon) + \frac{U^2}{\nu} f(\eta) g'(\upsilon) \\
\frac{\partial \omega_3}{\partial x_2} &= \frac{1}{\sqrt{\nu t}} f'(\eta) g(\upsilon) \quad \Rightarrow \quad \frac{\partial^2 \omega_3}{\partial x_2^2} = \frac{1}{\nu t} f''(\eta) g(\upsilon)\ .
\end{aligned} \tag{10.117}$$

Equation (10.114) reads now

$$-\frac{\eta}{2} f'(\eta) g(\upsilon) + \upsilon f(\eta) g'(\upsilon) = f''(\eta) g(\upsilon)\ . \tag{10.118}$$

Dividing through by (10.116) we get

$$\frac{\eta}{2} \frac{f'(\eta)}{f(\eta)} + \frac{f''(\eta)}{f(\eta)} = \upsilon \frac{g'(\upsilon)}{g(\upsilon)} = C\ . \tag{10.119}$$

If $g(0) \neq 0$ and $g'(0)$ is finite, then $C = 0$. This implies that $g'(\upsilon) = 0$ and thus $g(\upsilon)$ is constant.

- The f equation reads

$$f''(\eta) = -\frac{\eta}{2} f'(\eta) . \tag{10.120}$$

Integrating one obtains

$$f' = f'(0) e^{\frac{-\eta^2}{4}} . \tag{10.121}$$

Integrating again

$$f(\eta) = f(0) + f'(0) \int_0^\eta e^{\frac{-\zeta^2}{4}} d\zeta . \tag{10.122}$$

With the change of variable $\sigma = \frac{\zeta}{2}$, (10.122) becomes

$$f(\eta) = f(0) + 2 f'(0) \int_0^\eta e^{-\sigma^2} d\sigma . \tag{10.123}$$

Using the error function (3.79), we write

$$f(\eta) = f(0) + \sqrt{\pi} f'(0) \mathrm{erf}(\frac{\eta}{2}) . \tag{10.124}$$

- The thickness of the vortex sheet, i.e. the region where the vorticity does not vanish, increases like $\sqrt{\nu t}$.

10.5 Chapter Five

5.1 Hele-Shaw flow

- Inspection of (1.73) gives

$$\frac{\partial v_1}{\partial x_1} + \frac{\partial v_2}{\partial x_2} + \frac{\partial v_3}{\partial x_3} \simeq \frac{v_1}{L} + \frac{v_2}{L} + \frac{v_3}{h} \Rightarrow |v_3| \approx \varepsilon v_1 \simeq \varepsilon v_2 \ll |v_1| \simeq |v_2| . \tag{10.125}$$

- As the length scales in the directions parallel and orthogonal to the plates are quite different, we write

$$\left|\frac{\partial^2 v_1}{\partial x_1^2}\right| \approx \frac{v_1}{L^2} \ll \left|\frac{\partial^2 v_1}{\partial x_3^2}\right| \approx \frac{v_1}{\varepsilon^2 L^2}, \quad \left|\frac{\partial^2 v_2}{\partial x_1^2}\right| \approx \frac{v_2}{L^2} \ll \left|\frac{\partial^2 v_2}{\partial x_3^2}\right| \approx \frac{v_2}{\varepsilon^2 L^2} . \tag{10.126}$$

- The steady Stokes equations (1.73) and (2.54) reduce to the set

$$\frac{\partial v_i}{\partial x_i} = 0 \,, \tag{10.127}$$

$$\frac{\partial p}{\partial x_i} = \mu \nabla^2 v_i \,, \tag{10.128}$$

with $p = p(x_1, x_2)$ and $v_i = v_i(x_1, x_2)$, $i = 1, 2$. Since v_3 is of order ε, the $i = 3$ component of (2.54) indicates that the pressure is essentially constant across the gap and does not depend on x_3 as $\partial p/\partial x_3 = 0$, i.e., $p = p(x_1, x_2)$.

- This set of equations is meaningful in the symmetry plane parallel to the plates containing the origin of the coordinate axes. It is possible with the help of Eqs. (5.116) and (10.125)–(10.126) to write

$$v_i(x_1, x_2, x_3) = v_i(x_1, x_2, 0) f(x_3) \,, \tag{10.129}$$

as the variation of v_i with respect to x_1, x_2 is slower than that of f with respect to x_3.

- The Poiseuille flow solution (3.27) provides the relationship

$$f(x_3) = \left(1 - \frac{x_3^2}{h^2}\right) \,. \tag{10.130}$$

The momentum equations (10.128) become

$$\mu \frac{\partial^2 v_1}{\partial x_3^2} = \frac{\partial p}{\partial x_1} \,, \tag{10.131}$$

$$\mu \frac{\partial^2 v_2}{\partial x_3^2} = \frac{\partial p}{\partial x_2} \,. \tag{10.132}$$

- Taking Eqs. (10.129) and (10.130) into account, one obtains

$$v_i(x_1, x_2, 0) = -\frac{h^2}{2\mu}\frac{\partial p}{\partial x_i}, \quad \mathrm{i} = 1, 2 \,. \tag{10.133}$$

From (10.133) it is obvious that the velocity field is a gradient, is irrotational and hence, can be derived from a velocity potential. Introducing

$$v_i = \frac{\partial \varphi}{\partial x_i} \,, \tag{10.134}$$

Equation (10.133) yields

$$\varphi = -\frac{h^2 p}{2\mu} \,. \tag{10.135}$$

The streamline configuration will be the same in planes $x_3 = cst$. Furthermore they will be similar to those of a two-dimensional potential flow of an inviscid fluid around obstacles of the same shape. However near the obstacles the viscous fluid sticks to the walls, but this influence will be limited to a zone of thickness h. This discussion explains why the Hele-Shaw cell is used in many experiments to provide the observer with the geometrical pattern resulting from the presence of bodies inside an internal flow.

5.2 **Flow between parallel discs**

- With the velocity field given in Eq. (5.119), the continuity relation (A.20) gives

$$\frac{\partial v_\theta}{\partial \theta} = 0 \,, \tag{10.136}$$

showing that v_θ does not depend on θ.
The Navier–Stokes equations (A.21)–(A.23) reduce to

$$-\rho\frac{v_\theta^2}{r} = -\frac{\partial p}{\partial r} \tag{10.137}$$

$$0 = -\frac{1}{r}\frac{\partial p}{\partial \theta} + \mu\left[\frac{\partial}{\partial r}\left(\frac{1}{r}\frac{\partial}{\partial r}(r v_\theta)\right) + \frac{\partial^2 v_\theta}{\partial z^2}\right] \tag{10.138}$$

$$0 = -\frac{\partial p}{\partial z} + \rho b_z \,. \tag{10.139}$$

Because of the symmetry, the pressure term in (10.138) vanishes. Taking the particular form of (5.119) into account, Eq. (10.138) gives

$$f''(z) = 0 \,. \tag{10.140}$$

Integrating, we have $f(z) = C_1 z + C_2$. Imposing the boundary conditions

$$v_\theta(z = 0) = 0 \quad \text{and} \quad v_\theta(z = h) = \omega r \,, \tag{10.141}$$

we obtain $C_1 = \omega/h$ and $C_2 = 0$. Therefore the velocity field is

$$v_\theta = \frac{\omega}{h} r\, z \,. \tag{10.142}$$

- With (10.137), (10.139), (10.142) and $b_z = -g$, the pressure is

$$p(r, z) = -\rho g z + q(r) \,. \tag{10.143}$$

Setting $q(r) = 0$, Eq. (10.137) is satisfied provided $\omega \ll 1$ and $\partial p/\partial r = 0$.

- Throughout the fluid, the shear stress is

$$\sigma_{\theta z} = 2\mu d_{\theta z} = \mu \frac{\partial v_\theta}{\partial z} = \mu\omega \frac{r}{h} \,. \tag{10.144}$$

Consequently the moment M required to rotate the top disc, or to hold the bottom one still, is given by

$$M = \int_0^R (2\pi r)(r\sigma_{\theta z})dr = \frac{2\pi\mu\omega}{h}\int_0^R r^3 dr = \frac{\pi\mu\omega R^4}{2h} \,. \tag{10.145}$$

Since the quantities M, ω, a, h can presumably be measured, (10.145) can be used to determine the viscosity of the fluid, provided the underlying assumptions of creeping flow and idealized geometry are sufficiently well approximated.

10.6 Chapter Six

6.1

- The complex potential of the flow is

$$f(z) = m\,(\ln(z+1) + \ln(z-1) - \ln z) \tag{10.146}$$

corresponding to two sources located in $z = \pm 1$ and one sink in $z = 0$.
- The complex potential is expressed as

$$f(z) = m \ln\left(\frac{z^2-1}{z}\right) = m\left(\ln\left|\frac{z^2-1}{z}\right| + i\arg(\frac{z^2-1}{z})\right) = \varphi + i\psi \,. \tag{10.147}$$

- With $z = re^{i\theta}$, we obtain

$$\varphi = m\ln\left(\frac{1}{r}\sqrt{r^4 - 2r^2\cos(2\theta) + 1}\right) \tag{10.148}$$

and

$$\psi = m \arctan\left(\frac{r^2+1}{r^2-1}\tan\theta\right) \,. \tag{10.149}$$

Therefore the streamlines are

$$\psi = cst, \quad \text{with} \quad \frac{r^2+1}{r^2-1}\tan\theta = \alpha \tag{10.150}$$

with α constant. Let us notice that the Eq. (10.150) is invariant by the transformation $r \to 1/r$. Replacing r^2 by $x^2 + y^2$ and $\tan\theta$ by y/x, Eq. (10.150) becomes

$$(x^2 + y^2 + 1)y = \alpha(x^2 + y^2 - 1)x \quad (10.151)$$

which is invariant by the following symmetry $(x, y) \to (-x, -y)$. Consequently we can inspect the flow in the positive half-disk $r < 1$.

- The flow rate across the line joining the points $z_1 = \frac{1}{2}(1 + i)$ and $z_2 = 1/2$ is given with (6.12)

$$\begin{aligned} Q &= \psi(z_2) - \psi(z_1) \\ &= m \arctan\left(\frac{r_2^2 + 1}{r_2^2 - 1} \tan\theta_2\right) - m \arctan\left(\frac{r_1^2 + 1}{r_1^2 - 1} \tan\theta_1\right) \\ &= m \arctan(3) \end{aligned} \quad (10.152)$$

as $r_2 = 1/2$, $\theta_2 = 0$, $r_1 = \sqrt{2}/2$ and $\theta_1 = \pi/4$.

6.2

- The singularities are located in

$$z_{1,1'} = \pm 1 \quad (10.153)$$

$$z_{2,2'} = \pm 2i \quad (10.154)$$

$$z_3 = 0\,. \quad (10.155)$$

- They are all inside the circle $C : x^2 + y^2 = 9$. The complex circulation $\mathbf{\Gamma}$ defined by (6.22) allows for the computation of the flow rate across C and the circulation around the circle

$$\begin{aligned} \mathbf{\Gamma} &= \int_C df, \quad z = 3e^{i\theta} \\ &= \int_0^{2\pi} df = f(3e^{i2\pi}) - f(3) \\ &= (1 + i)\left(\ln 8e^{i4\pi} - \ln 8\right) + (2 - 3i)\left(\ln 13e^{i4\pi} - \ln 13\right) \\ &+ \frac{e^{-i2\pi}}{3} - \frac{1}{3} \\ &= 4\pi i\,((1 + i) + (2 - 3i)) = 8\pi + 12\pi i\,. \end{aligned} \quad (10.156)$$

Then $Q = 12\pi$ and $\Gamma = 8\pi$.

6.3

- With the relation (6.156) we calculate

$$\begin{aligned} z = \cosh f &= \frac{e^f + e^{-f}}{2} = \frac{1}{2}\left(e^{\varphi + i\psi} + e^{-(\varphi + i\psi)}\right) \\ 2x + 2iy &= e^{\varphi}(\cos\psi + i\sin\psi) + e^{-\varphi}(\cos\psi - i\sin\psi)\,. \end{aligned} \quad (10.157)$$

Separating the real and imaginary contributions, we have

$$2x = e^{\varphi}\cos\psi + e^{-\varphi}\cos\psi = \cos\psi(e^{\varphi} + e^{-\varphi})$$
$$2y = e^{\varphi}\sin\psi + e^{-\varphi}\sin\psi = \sin\psi(e^{\varphi} - e^{-\varphi}) ,$$

and

$$x = \cosh\varphi\cos\psi, \quad y = \sinh\varphi\sin\psi . \tag{10.158}$$

Therefore one has

$$\left(\frac{x}{\cosh\varphi}\right)^2 + \left(\frac{y}{\sinh\varphi}\right)^2 = 1 \tag{10.159}$$
$$\left(\frac{x}{\cos\psi}\right)^2 - \left(\frac{y}{\sin\psi}\right)^2 = 1 . \tag{10.160}$$

Equations (10.159) and (10.160) show that the equipotentials are ellipses and streamlines hyperbolas that are drawn in Fig. 10.6. Note that for $y = 0$, there is no solution for $|x| > 1$.

- Let us evaluate the velocity for $y = 0$ and $-1 \le x \le 1$. Obviously by symmetry, $u = 0$. From (6.14) we have

$$\frac{dz}{df} = \frac{1}{w} = \frac{1}{u - iv} = \sinh f = \sqrt{\cosh^2 f - 1} = \sqrt{z^2 - 1} . \tag{10.161}$$

Therefore

$$u - iv = \frac{1}{\sqrt{z^2 - 1}} = \frac{1}{\sqrt{x^2 - 1}} = \frac{-i}{\sqrt{1 - x^2}} . \tag{10.162}$$

Consequently $v = -i/\sqrt{1 - x^2}$. Note the $|v| = \infty$ for $x = \pm 1$ and $|v| = 1$ for $x = 0$.

6.4 Flow in front of a circular obstacle

- The complex potential $g(\zeta)$ may be decomposed as a sum of noteworthy terms

$$g(\zeta) = \frac{Q}{2\pi}\left(\ln(\zeta - a) + \ln(\zeta + a) - \ln(\zeta - 1) - \ln(\zeta + 1)\right) . \tag{10.163}$$

The flow is thus created by two sources situated in $\zeta = \pm a$ and by two sinks in $\zeta = \pm 1$. The two images are the images of the singularities with respect to the wall, namely the η axis.

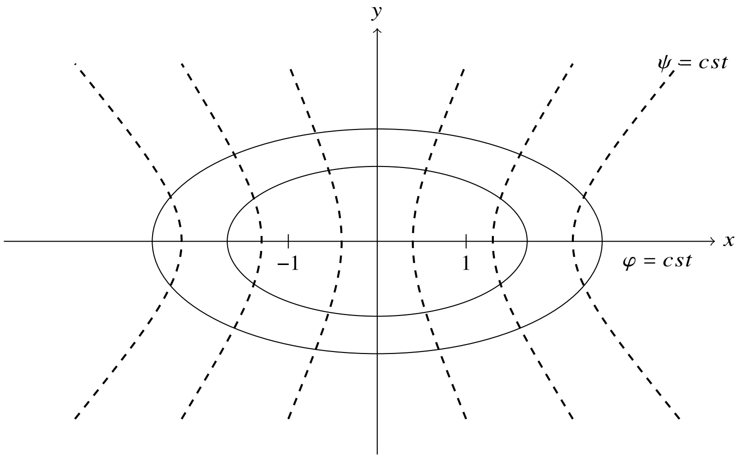

Fig. 10.6 Streamlines and equipotentials for $z = \cosh f$

- The complex velocity reads

$$w_\zeta = \frac{dg(\zeta)}{d\zeta} = \frac{Q}{2\pi}\left(\frac{1}{\zeta - a} + \frac{1}{\zeta + a} - \frac{1}{\zeta - 1} - \frac{1}{\zeta + 1}\right)$$
$$= \frac{Q}{2\pi}\left(\frac{2\zeta(a^2 - 1)}{(\zeta^2 - a^2)(\zeta^2 - 1)}\right) . \quad (10.164)$$

- With the conformal mapping (6.158), the wall $\xi = 0$ in the ζ plane is transformed in a circle of unit radius in the z plane as we have

$$x + iy = \frac{1 + i\eta}{1 - i\eta} \quad \Rightarrow \quad x^2 + y^2 = 1 . \quad (10.165)$$

- Introducing successively in $g(\zeta)$ the positions of the two sources and the two sinks, $\zeta = \pm a$ and $\zeta = \pm 1$ respectively, with the definition of b, we obtain that the source in $\zeta = a$ becomes a source in $x = b$, the image source in $\zeta = -a$ yields a source in $x = 1/b$, the sink in $\zeta = 1$ gives a sink at infinity, and eventually, the image sink in $\zeta = -1$ generates the sink in $z = 0$.
- Therefore the image of the half plane $\xi \geq 0$ in the z plane is the exterior of the unit circle centered at the origin as shown in Fig. 10.7.
- The complex velocity $w(z)$ in the z plane is

$$w = w_\zeta\left(\frac{z - 1}{z + 1}\right) \quad (10.166)$$

- The complex potential in the z plane is made of two sources and one sink

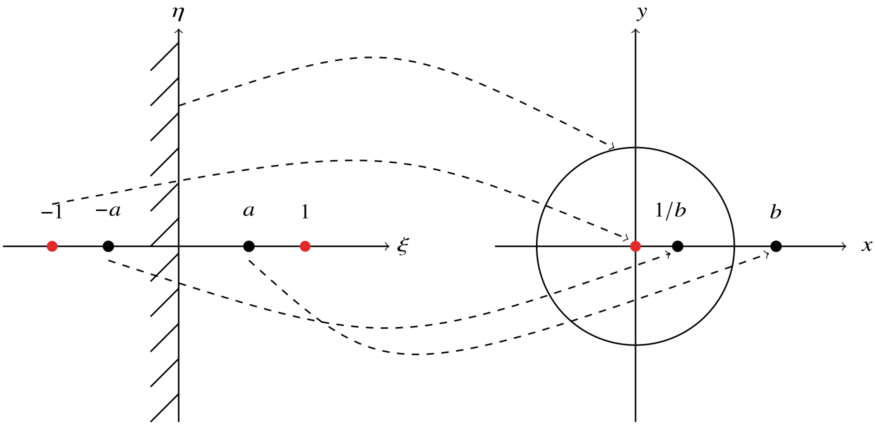

Fig. 10.7 Source in front of a circular obstacle with $a < 1$. Red dots are sinks and black dots sources

$$f(z) = \frac{Q}{2\pi}\left(\ln(z-b) + \ln(z-\frac{1}{b}) - \ln z\right) \qquad (10.167)$$

which is exactly Eq. (6.159).

6.5 Flow over a forward facing step

- For the half line $\xi \geq 0$ and $\eta = 0$ we have $\arg dz - \arg d\zeta = (\arg\xi - \arg(\xi + a))/2 = 0$.
- For the AO segment, one has $\arg dz - \arg d\zeta = (\arg\xi - \arg(\xi + a))/2 = \pi/2$ and for $\xi < -a$, $\arg dz - \arg d\zeta = (\arg\xi - \arg(\xi + a))/2 = 0$. The geometry of the transformed domain is a forward facing step as shown in Fig. 10.8.
- The velocity in the physical plane is

$$w = g'(\zeta)\frac{d\zeta}{dz} = U\left(\frac{\zeta + a}{\zeta}\right)^{1/2}. \qquad (10.168)$$

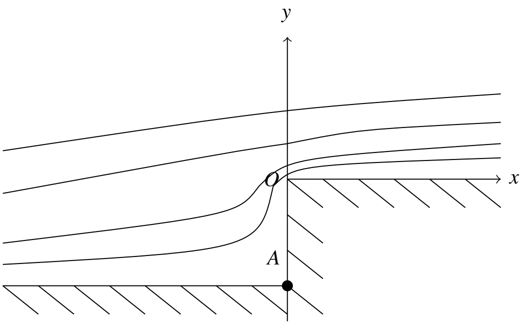

Fig. 10.8 Sketch of the flow over a forward facing step

In the limit $\eta \to 0$, we have

$$w = U\left(\frac{\xi + a}{\xi}\right)^{1/2} . \tag{10.169}$$

We notice that for $\xi = -a$, the velocity vanishes and this point is indeed a stagnation point; in $\xi = 0$, the velocity goes to infinity.

More details for this problem may be found in Sect. 10.6 of Milne-Thompson [59].

10.7 Chapter Seven

7.1 The boundary conditions are given by

$$x_2 = 0 \; : \; v_1 = v_2 = 0 \tag{10.170}$$

$$x_2 = \delta_\infty \; : \; v_1 = U_e(x_1), \; \frac{\partial v_1}{\partial x_2} = \frac{\partial^2 v_1}{\partial x_2^2} = 0 \, . \tag{10.171}$$

From the Navier–Stokes equations, we get

$$\nu \frac{\partial^2 v_1}{\partial x_2^2} = \frac{1}{\rho}\frac{\mathrm{d}p_e}{\mathrm{d}x_1} = -U_e \frac{\mathrm{d}U_e}{\mathrm{d}x_1}. \tag{10.172}$$

With the help of Eqs. (10.171) and (10.172), we calculate the coefficients a, b, c and d. With the substitution

$$\lambda = \frac{\delta_\infty^2}{\nu}\frac{dU_e}{dx_1}, \tag{10.173}$$

we find

$$a = \tfrac{\lambda}{6} + 2, \tag{10.174}$$

$$b = -\tfrac{\lambda}{2}, \tag{10.175}$$

$$c = \tfrac{\lambda}{2} - 2, \tag{10.176}$$

$$d = 1 - \tfrac{\lambda}{6}. \tag{10.177}$$

The velocity profile is then written

$$v_1/U_e = 2s - 2s^3 + s^4 + \frac{\lambda}{6}s(1-s)^3. \tag{10.178}$$

In the present case, the outer velocity is constant ($U_e = \text{cst}$). Therefore $\lambda = 0$ and the velocity profile is simplified

$$\frac{u}{U_e} = 2s - 2s^3 + s^4. \tag{10.179}$$

The displacement thickness δ^* is

$$\delta^* = \int_0^\delta \mathrm{d}x_2 \left(1 - \frac{v_1}{U_e}\right) = \frac{3}{10}\delta_\infty. \tag{10.180}$$

For the momentum thickness θ, we have the definition

$$\theta = \int_0^\delta \mathrm{d}x_2 \left[\frac{v_1}{U_e}\left(1 - \frac{v_1}{U_e}\right)\right] = \frac{37}{315}\delta_\infty. \tag{10.181}$$

The wall shear stress τ_w is given by

$$\tau_w = -\int_0^{\delta_\infty} \mathrm{d}x_2 \frac{\partial}{\partial x_2}\left(\frac{\partial v_1}{\partial x_2}\right) = 2\mu\frac{U_e}{\delta_\infty}. \tag{10.182}$$

Finally, through the von Kármán equation (7.89), we have a relation between τ_w and θ

$$\frac{d\theta}{dx_1} = \frac{\tau_w}{\rho U_e^2}. \tag{10.183}$$

Substituting the above expressions for θ and τ_w, one finds

$$\frac{37}{315}\frac{d\delta}{dx_1} = \frac{2\nu}{\delta U_e} \Rightarrow \delta_\infty = 2\sqrt{\frac{315}{37}}\sqrt{\frac{\nu x_1}{U_e}} = 5.83\sqrt{\frac{\nu x_1}{U_e}}. \tag{10.184}$$

7.2 Referring to Fig. 7.5, the problem solution is performed through the next steps.

- The boundary conditions for the boundary layer developing over the flat plate are
  1. No slip wall
  $$v_1(0) = 0 \quad \text{for} \quad x_2 = 0\,. \tag{10.185}$$
  2. Matching condition with the outer flow field at $x_2 = \delta_0$
  $$v_1(\delta_0) = U \quad \text{for} \quad x_2 = \delta_0\,. \tag{10.186}$$
  3. Stress condition at $x_2 = \delta_0$
  $$\frac{\partial v_1}{\partial x_2} = 0 \quad \text{for} \quad x_2 = \delta_0\,. \tag{10.187}$$

- Evaluation of A, B, C.

1. Equation (10.185) implies $C = 0$.
2. Condition (10.187) imposes

$$AB\cos(Bx_2)\big|_{x_2=\delta_0} = 0 \quad \Rightarrow B = \frac{\pi}{2\delta_0}\,. \tag{10.188}$$

3. Condition (10.186) gives $A = U$. The velocity profile is therefore

$$v_1(x_2) = U\sin\left(\frac{\pi x_2}{2\delta_0}\right)\,. \tag{10.189}$$

- Computation of θ

1. Introducing the variable $s = x_2/\delta_0$, the momentum thickness becomes

$$\begin{aligned}\theta &= \delta_0\int_0^1 \sin(\frac{\pi}{2}s)\left(1-\sin(\frac{\pi}{2}s)\right)ds\\ &= \delta_0(\frac{2}{\pi}-\frac{1}{2}) = 0.1366\,\delta_0\,.\end{aligned} \tag{10.190}$$

2. Continuity over the control volume

$$-\int_0^{\delta_0}\rho U dx_2 + \int_0^{\delta_0}\rho v_1 dx_2 + \int_0^{x}\rho v_2'\,dx' = 0\,. \tag{10.191}$$

Note that the third integral on the left-hand side of (10.191) takes care of the mass flow rate $\Delta\dot{m}$ across the upper boundary of the control volume. Equation (10.191) leads to the relation

$$\int_o^{x}\rho v_2' dx' = \int_0^{\delta_0}\rho(U-v_1)dx_2\,. \tag{10.192}$$

3. Integral momentum equation over the control volume

$$-\int_0^{\delta_0}\rho U^2 dx_2 + \int_0^{\delta_0}\rho v_1^2 dx_2 + \int_0^{x}\rho v_2' U dx' = -\int_0^{x}\tau_w(x')dx'\,. \tag{10.193}$$

Combining (10.193) with (10.192), one gets

$$-\int_0^{\delta_0}\rho(U^2-v_1^2)dx_2 + \int_0^{\delta_0}\rho U(U-v_1)dx_2 = -\int_0^{x}\tau_w(x')dx'\,. \tag{10.194}$$

Then

$$\int_0^{\delta_0}\rho v_1(v_1-U)dx_2 = -\int_0^{x}\tau_w(x')dx'\,. \tag{10.195}$$

From (10.195) we obtain

$$\tau_w = -\frac{d}{dx}\int_0^{\delta_0} \rho v_1(v_1 - U)dx_2 = \frac{d\theta}{dx}\rho U^2 \, . \tag{10.196}$$

Consequently

$$\frac{d\theta}{dx_1} = \frac{\tau_w}{\rho U^2} \, . \tag{10.197}$$

4. Computation of τ_w

$$\tau_w = \mu \frac{\partial v_1}{\partial x_2}\Big|_{x_2=0} = \frac{\mu U \pi}{2\delta_0}\cos(\frac{\pi x_2}{2\delta_0})\Big|_{x_2=0} = \frac{\mu U \pi}{2\delta_0} \, . \tag{10.198}$$

5. Computation of δ_0.
   Using (10.197), (10.198) and (10.190) we have

$$\frac{d\theta}{dx_1} = \frac{\mu\pi}{2\rho U \delta_0}$$

$$0.1366\frac{d\delta_0}{dx_1} = \frac{\mu\pi}{2\rho U \delta_0} \, . \tag{10.199}$$

   Integrating (10.199) one has

$$\delta_0 = 4.795\sqrt{\frac{\nu x_1}{U}} \, , \tag{10.200}$$

   result that should be compared with (7.58).

7.3

- At some distance from the leading edge, the boundary layer is constant in shape and thickness. As a consequence, we have

$$\frac{\partial v_1}{\partial x_1} = 0 \, . \tag{10.201}$$

  From the continuity equation and (10.201), one gets

$$\frac{\partial v_2}{\partial x_2} = 0 \quad \Rightarrow \quad v_2 = cst = V \, . \tag{10.202}$$

  Prandlt's equation (7.40) with (10.202) becomes

$$V\frac{\partial v_1}{\partial x_2} = \nu \frac{\partial^2 v_1}{\partial x_2^2} \, . \tag{10.203}$$

This second-order differential equation has for solution

$$v_1 = Ae^{\frac{V}{\nu}x_2} + B\ . \tag{10.204}$$

The boundary condition at the plate imposes $v_1 = 0$ at $x_2 = 0$, giving $B = -A$. At $x_2 = \infty$, we have $v_1 = U_\infty$. Recalling that $V < 0$ one has $A = U_\infty$. Therefore the velocity profile reads

$$\frac{v_1}{U_\infty} = 1 - e^{\frac{V}{\nu}x_2}\ . \tag{10.205}$$

- The wall shear stress is

$$\tau_w = \mu\frac{\partial v_1}{\partial x_2}\Big|_{x_2=0} = -\mu(\frac{V}{\nu}U) = -\rho V U_\infty\ . \tag{10.206}$$

  Observe that τ_w does not depend on the viscosity.
- The displacement thickness (7.59) with (10.204) gives

$$\delta^* = -\frac{\nu}{V}\ . \tag{10.207}$$

  while the momentum thickness (7.63) becomes

$$\theta = -\frac{\nu}{2V}\ . \tag{10.208}$$

  Finally the shape factor H is

$$H = \frac{\delta^*}{\theta} = 2\ . \tag{10.209}$$

  to be compared to $H = 8/3$ for the non-porous plate.

10.8 Chapter Eight

8.1 The spiral flow is the same as the helical flow solved in Sect. 3.2.3. The Couette solution (3.41) will be denoted by $V(r)$ while the axial solution (3.64) corresponding to the Poiseuille flow in the annular section is referred to as $W(r)$. The axisymmetric Navier–Stokes equations are given by (8.27)–(8.30). The stability analysis rests upon a base flow and three-dimensional axisymmetric perturbations. We have

$$\boldsymbol{v} = (u, V + v, W + w) \quad \text{and} \quad p = P + p_p\ . \tag{10.210}$$

We carry out a linearization of the governing equations discarding the second-order terms of the perturbations. We get

$$\rho\left(\frac{\partial u}{\partial t}+(W+w)\frac{\partial u}{\partial z}-\frac{(V+v)^2}{r}\right)=-\frac{\partial(P+p_p)}{\partial r}+\mu(\Delta u-\frac{u}{r^2}) \quad (10.211)$$

$$\rho\left(\frac{\partial v}{\partial t}+u\frac{dV}{dr}+(W+w)\frac{\partial v}{\partial z}+\frac{u}{r}(V+v)\right)=\mu(\Delta v-\frac{v}{r^2}) \quad (10.212)$$

$$\rho\left(\frac{\partial w}{\partial t}+u\frac{\partial(W+w)}{\partial r}+W\frac{\partial w}{\partial z}\right)=-\frac{\partial(P+p_p)}{\partial z}+\mu\Delta w \quad (10.213)$$

$$\frac{\partial u}{\partial r}+\frac{u}{r}+\frac{\partial w}{\partial z}=0\,. \quad (10.214)$$

As the base flow satisfies the Navier–Stokes equations, a further step in the linearization brings the equations

$$\rho\left(\frac{\partial u}{\partial t}+W\frac{\partial u}{\partial z}-\frac{2Vv}{r}\right)=-\frac{\partial p_p}{\partial r}+\mu(\Delta u-\frac{u}{r^2}) \quad (10.215)$$

$$\rho\left(\frac{\partial v}{\partial t}+u(\frac{V}{r}+\frac{dV}{dr})+W\frac{\partial v}{\partial z}\right)=\mu(\Delta v-\frac{v}{r^2}) \quad (10.216)$$

$$\rho\left(\frac{\partial w}{\partial t}+u\frac{dW}{dr}+W\frac{\partial w}{\partial z}\right)=-\frac{\partial p_p}{\partial z}+\mu\Delta w \quad (10.217)$$

$$\frac{\partial u}{\partial r}+\frac{u}{r}+\frac{\partial w}{\partial z}=0\,. \quad (10.218)$$

Using the normal modes (8.40) and the notation (8.41), the stability equations are

$$\sigma\hat{u}+ikW\hat{u}-\frac{2V\hat{v}}{r}=-\frac{1}{\rho}D\hat{p}_p+\nu(DD_*-k^2)\hat{u} \quad (10.219)$$

$$\sigma\hat{v}+\hat{u}D_*V+ikW\hat{v}=\nu(DD_*-k^2)\hat{v} \quad (10.220)$$

$$\sigma\hat{w}+\hat{u}\frac{dW}{dr}+ikW\hat{w}=-ik\frac{\hat{p}_p}{\rho}+\nu(D_*D-k^2)\hat{w} \quad (10.221)$$

$$D_*\hat{u}+ik\hat{w}=0\,. \quad (10.222)$$

Extracting $\hat{w}$ from Eq. (10.222) and inserting this expression in (10.221), we obtain

$$\frac{\hat{p}_p}{\rho}=\frac{1}{k^2}\left[\nu(D_*D-k^2)-\sigma-ikW\right]D_*\hat{u}+\frac{i\hat{u}}{k}\frac{dW}{dr}\,. \quad (10.223)$$

Taking the derivative D of (10.223) and using it in (10.219) we are left with the relations

$$\nu\left(DD_*-k^2\right)^2\hat{u}-2k^2\frac{V}{r}\hat{v}+ik^3\hat{u}W+\frac{i\hat{u}r}{k}\left(\frac{W'}{r}\right)'=\sigma(DD_*-k^2)\hat{u} \quad (10.224)$$

$$\nu\left(DD_*-k^2\right)\hat{v}-(D_*V)\hat{u}-ik\hat{v}W=\sigma\hat{v} \quad (10.225)$$

$$\hat{u}=\hat{v}=D\hat{u}=0 \quad \text{for} \quad r=R_1,R_2\,. \quad (10.226)$$

The interested reader may find in Ng and Turner [62] the numerical results obtained by the compound matrix method for the stability of the spiral flow under axisymmetric disturbances for the small gap approximation. This analysis sheds light on the interaction of centrifugal and shear instabilities.

8.2 **Rayleigh–Bénard instability**

The solution follows the development proposed by Chandrasekhar [18] and Drazin [26].

- The velocity of the base flow is zero $\boldsymbol{v} = 0$. The temperature profile is linear as it is solution of $d^2T_C/dx_2^2 = 0$, with the boundary conditions $T_C = T_0$ for $x_2 = 0$ and $T_C = T_1$ for $x_2 = d$. The lower index C indicates the conductive nature of the solution. Hence
$$T_C = T_0 - \frac{T_0 - T_1}{d} x_2 \,. \tag{10.227}$$
The hydrostatic pressure p_{hyd} is obtained from the Navier–Stokes equation (1.116) that yields
$$0 = -\nabla p \; + +\rho_0((1 - \alpha(T - T_0))\boldsymbol{g} \,, \tag{10.228}$$
and consequently using (10.227)
$$p_{hyd} = p_0 - \rho g(x_2 + \alpha \frac{T_0 - T_1}{d} \frac{x_2^2}{2}) \,. \tag{10.229}$$
- For the sake of facility, the dimensionless quantities are denoted without primes in the sequel. The velocity perturbations are $\boldsymbol{v} = (u, v, w)$. Using (8.67), the linearized equations are
$$\operatorname{div} \boldsymbol{v} = 0, \tag{10.230}$$
$$\frac{\partial \boldsymbol{v}}{\partial t} = -\nabla p_p \; + \; Pr \triangle \boldsymbol{v} + Ra Pr \, T \boldsymbol{g}', \tag{10.231}$$
$$\frac{\partial T}{\partial t} - v = \triangle T. \tag{10.232}$$
- The **curl** of the velocity generates the vorticity (1.40). The dimensionless gravity vector of unit length acts in the vectorial $\boldsymbol{k}$ direction. Then we have taking (1.41) into account
$$\mathbf{curl}(T\boldsymbol{k}) = \varepsilon_{ijk} \frac{\partial T}{\partial x_j} e_k = \nabla T \times \boldsymbol{k} \,. \tag{10.233}$$
The resulting equation reads
$$\frac{\partial \boldsymbol{\omega}}{\partial t} = Ra \, Pr \nabla T \times \boldsymbol{e}_k + Pr \triangle \boldsymbol{\omega} \,. \tag{10.234}$$

- The application of **curl** to Eq. (10.234) leads to the relationship

$$\frac{\partial \triangle \boldsymbol{v}}{\partial t} = Ra\ Pr \left(\triangle T \boldsymbol{e}_i - \boldsymbol{\nabla}(e_j \frac{\partial T}{\partial x_j}) \right) + Pr \triangle\triangle \boldsymbol{v} \ . \tag{10.235}$$

To obtain (10.235) the following computation is needed

$$\begin{aligned} \mathbf{curl}(\boldsymbol{\nabla} T \times \boldsymbol{e}_k)_i &= \varepsilon_{ijk}\varepsilon_{klm} \frac{\partial^2 T}{\partial x_l \partial x_j} e_m \\ &= (\delta_{il}\delta_{jm} - \delta_{im}\delta_{jl}) \frac{\partial^2 T}{\partial x_l \partial x_j} e_m \\ &= e_j \frac{\partial^2 T}{\partial x_j \partial x_i} - e_i \triangle T \ . \end{aligned} \tag{10.236}$$

- The x_2 component of (10.235) is

$$\begin{aligned} \frac{\partial \triangle v}{\partial t} &= Ra\ Pr \left(\triangle T - \frac{\partial^2 T}{\partial x_2^2} \right) + Pr \triangle\triangle v \\ &= Ra\ Pr \triangle_H T + Pr \triangle\triangle v \ , \end{aligned} \tag{10.237}$$

where $\triangle_H = \partial^2/\partial x_1^2 + \partial^2/\partial x_3^2$ is the horizontal Laplacian.
- Let us eliminate T between (10.232) and (10.237). From (10.232) we compute

$$T = \left(\frac{\partial}{\partial t} - \triangle \right)^{-1} v \ . \tag{10.238}$$

Plugging (10.238) in (10.237) one gets

$$\left(\frac{\partial}{\partial t} - \triangle \right) \left(\frac{1}{Pr}\frac{\partial}{\partial t} - \triangle \right) \triangle v = Ra \triangle_H v \ . \tag{10.239}$$

The boundary conditions are

$$v = \frac{\partial v}{\partial x_2} = T = 0 \quad \text{for} \quad x_2 = 0 \quad \text{and} \quad x_2 = d. \tag{10.240}$$

- We choose the normal modes in horizontal Fourier space

$$T = \Theta(x_2) e^{\sigma t + i(k_1 x_1 + k_3 x_3)} \tag{10.241}$$

$$v = V(x_2) e^{\sigma t + i(k_1 x_1 + k_3 x_3)} \ . \tag{10.242}$$

Substitution of (10.241)–(10.242) in (10.232) and (10.237) produces

$$(D^2 - k^2 - \sigma)T = -W \tag{10.243}$$

$$(D^2 - k^2)(D^2 - k^2 - \frac{\sigma}{Pr})W = k^2 RaT \ , \tag{10.244}$$

with $D = d/dx_2$ and $k^2 = k_1^2 + k_3^2$.
Elimination of T between (10.243) and (10.244) yields a sixth-order differential equation

$$(D^2 - k^2)(D^2 - k^2 - \sigma)(D^2 - k^2 - \frac{\sigma}{Pr})W = -k^2 RaW \ , \tag{10.245}$$

with the boundary conditions $W = DW = T = 0$ at $x_2/d = 0, 1$.

The problem is solved numerically by a spectral method, see e.g. [23]. The critical Rayleigh number in the case of rigid conducting plates is $Ra_{crit} = 1708$ with $k_{crit} = 3.117$.

10.9 Chapter Nine

9.1 Taking the conjugate complex of (9.52) one has

$$f^*(\boldsymbol{x}) = \sum_{\boldsymbol{k}'} \hat{f}^*(\boldsymbol{k}') e^{i\boldsymbol{k}'\cdot\boldsymbol{x}} \ . \tag{10.246}$$

Setting $\boldsymbol{k}' = -\boldsymbol{k}$, one obtains

$$f^*(\boldsymbol{x}) = \sum_{\boldsymbol{k}} \hat{f}^*(-\boldsymbol{k}) e^{-i\boldsymbol{k}\cdot\boldsymbol{x}} \ . \tag{10.247}$$

As f is real, we conclude that $f^* = f$ and the relation (9.53).

9.2 With the definition (9.60), we write

$$Q_{ij}(-\boldsymbol{r}) = \overline{v_i'(\boldsymbol{x})v_j'(\boldsymbol{x}-\boldsymbol{r})} \ . \tag{10.248}$$

If we have now $\boldsymbol{x} = \boldsymbol{x}' + \boldsymbol{r}$, the former relation yields

$$Q_{ij}(-\boldsymbol{r}) = \overline{v_i'(\boldsymbol{x}'+\boldsymbol{r})v_j'(\boldsymbol{x}')} = Q_{ji}(\boldsymbol{r}) \ . \tag{10.249}$$

Symmetry is then proved.

9.3 The use of Eq. (9.241) requires the following algebraic expansions

$$(I_d - G)^3 = I_d - 3G + 3G^2 - G^3 \tag{10.250}$$

$$(I_d - G)^4 = I_d - 4G + 6G^2 - 4G^3 + G^4 \tag{10.251}$$

$$(I_d - G)^5 = I_d - 5G + 10G^2 - 10G^3 + 5G^4 - G^5 \,. \tag{10.252}$$

Then

$$Q_3 = \sum_{n=0}^{3}(I_d - G)^n = 4I_d - 6G + 4G^2 - G^3 \tag{10.253}$$

$$Q_5 = \sum_{n=0}^{5}(I_d - G)^n = 6I_d - 15(G + G^3) + 20G^2 + 6G^4 - G^5. \tag{10.254}$$

From (10.253) and (10.254), we recover easily the relations (9.243) and (9.244).